Cargo transportation by two species of motor protein

Yunxin Zhang

Phys. Rev. E **87**, 052705 — Published 10 May 2013
DOI: 10.1103/PhysRevE.87.052705

Cargo transportation by two species of motor protein

Yunxin Zhang*

Shanghai Key Laboratory for Contemporary Applied Mathematics,

Laboratory of Mathematics for Nonlinear Science, Centre for Computational Systems Biology,

School of Mathematical Sciences, Fudan University, Shanghai 200433, China.

(Dated: April 26, 2013)

The cargo motion in living cells transported by two species of motor protein with different intrinsic directionality is discussed in this study. Similar to single motor movement, cargo steps forward and backward along microtubule stochastically. Recent experiments found that, cargo transportation by two motor species has a memory, it does not change its direction as frequently as expected, which means that its forward and backward step rates depends on its previous motion trajectory. By assuming cargo has only the least memory, i.e. its step direction depends only on the direction of its last step, two cases of cargo motion are detailed analyzed in this study: **(I)** cargo motion under constant external load; and **(II)** cargo motion in one fixed optical trap. Due to the existence of memory, for the first case, cargo can keep moving in the same direction for a long distance. For the second case, the cargo will oscillate in the trap. The oscillation period decreases and the oscillation amplitude increases with the motor forward step rates, but both of them decrease with the trap stiffness. The most likely location of cargo, where the probability of finding the oscillated cargo is maximum, may be the same as or may be different with the trap center, which depends on the step rates of the two motor species. Meanwhile, if motors are robust, i.e. their forward to backward step rate ratios are high, there may be two such most likely locations, located on the two sides of the trap center respectively. The probability of finding cargo in given location, the probability of cargo in forward/backward motion state, and various mean first passage times of cargo to give location or given state are also analyzed.

PACS numbers:

Keywords: cargo memory; tug-of-war; motor protein

I. INTRODUCTION

Motility is one of the basic properties of living cells, in which cargos, including organelles and vesicles, are usually transported by cooperation of various motor proteins [1, 2], such as the plus-end directed kinesin and minus-directed dynein [3–5]. Experiments found that, using the energy released in ATP hydrolysis [6–9], these motors can move processively along microtubule with step size 8 nm and in hand-over-hand manner [10–12].

Although numerous experimental and theoretical studies have been done to understand this cargo transportation process, so far the mechanism of which is not fully clear. In [13], one basic model is presented by assuming cargo is transported by only one type of motors and all the motors share the external load equally. Then in [14], one more

*Email: xyz@fudan.edu.cn

realistic tug-of-war model is designed, in which the cargo is assumed to be transported by two types of motors with opposite intrinsic directionality, and motors can reverse their motion direction under large external load. According to some experimental phenomena this tug-of-war model seems reasonable [15, 16]. In either of the models given in [13, 14], the only interaction among different motors is that, motors from the same type share load equally and motors from different types act as load to each other. In [17–19], some complicated models are presented, in which interactions among motors are described by linear springs. Recent experiments found that the tug-of-war model might not be reasonable enough to explain some experimental phenomena, so several new models are designed to try to understand the mechanism of cargo motion by multiple motors [20–26]. Finally, more discussion about cargo transportation in cells can be found in [27–35].

In recent experiment [36], by measuring cargo dynamics in optical trap, Leidel *et al.* found cargo motion along microtubule has memory. Cargo is more likely to resume motion in the same direction rather than the opposite one. This finding implies that, cargo location in the next time depends not only on its present location but also on how it reaches the present location. The behavior of cargo depends on its motion trajectory, which is different from the assumptions in previous models. In this study, one model for cargo motion with memory will be presented. But for simplicity, we assume that the cargo has only a little memory, it can only remember the motion direction in its last step.

II. MODEL FOR CARGO MOTION WITH MEMORY

In this study, the cargo is assumed to be tightly bound by two types of motor proteins: *plus-end* (or *forward*) motors and *minus-end* (or *backward*) motors. The forward and backward step rates of each *plus-end* motor are u and w, and the forward and backward step rates of each *minus-end* motor are f and b. Obviously $u \gg w$ but $b \gg f$ when the external load is low, since the intrinsic directionalities of motors from the two different types are opposite to each other, and the intrinsic motion direction of *plus-end* motor is plus-end directed (i.e. to the plus-end of microtubule), but the intrinsic motion direction of *minus-end* motor is minus-end directed (i.e. to the minus-end of microtubule). By assuming that all motors from the same type share the load equally, we only need to discuss the simplest cases in which the cargo is transported by only one *plus-end* motor and one *minus-end* motor. For example, if there are k *plus-end* motors, the total external load is F_c, the forward and backward step rates of one single *plus-end* motor are u_c and w_c, and the motor step size is l_c. Then these k *plus-end* motors can be effectively replaced by one single *plus-end* motor with load $F = F_c/k$, step rates $u = ku_c$ and $w = kw_c$, and step size $l_0 = l_c/k$. Since the experiments in [36] showed that, the number of motors moving the cargo is usually the same in both directions, this study also assumes the step sizes of the *plus-end* motor and *minus-end* motor are the same (note, the step size of single *plus-end* motor kinesin and step size of single *minus-end* motor dynein are the same $l_0 \approx 8$ nm [2, 9, 12]).

This study will mainly discuss two special cases: **(I)** Cargo moves under constant external load. *In vitro*, this constant load may be applied by one feedback optical trap, or *In vivo*, this constant load may be from the viscous environment with invariable drag coefficient. **(II)** Cargo moves in one fixed optical trap, this case is easy to be performed experimentally, and so the corresponding theoretical results are easy to be verified.

A. Cargo Motion under constant load

For the sake of convenience, the cargo is said to be in *plus-state* n^+ if it reached its present location n by one forward step from location $n-1$. Similarly, the cargo is said to be in minus-state n^- if its previous step is minus-end directed, see Fig. 1(a) for the schematic depiction. In *plus-state*, the forward step rate is higher than backward step rate $u > w$, but in *minus-state* the forward step rate is lower than backward step rate $f < b$. So in *plus-state*, the cargo is more likely to move forward, but in *minus-state*, the cargo will be more likely to move backward. For example, for a cargo in location n, if its previous step is plus-end directed, from either *plus-state* $n^+ - 1$ or *minus-state* $n^- - 1$ to location n, then in the next step the cargo will be more likely to move to location $n+1$ (*plus-state* $n^+ + 1$), since the cargo is now in plus-state n^+ and its forward step rate u is higher than its backward step rate w. On the contrary, if it got to its present location n from location $n+1$ (either from *plus-state* $n^+ + 1$ or from *minus-state* $n_- + 1$), then in the next step the cargo will be more likely to move to location $n-1$ (*minus-state* $n^- - 1$), since the cargo is now in *minus-state* n^- and its backward step rate b is higher than its forward step rate f. This behavior means that the cargo can remember its motion direction of its last step.

Let p, ρ be probabilities of cargo in *plus-state* and *minus-state* respectively, then

$$dp/dt = f\rho - wp = -d\rho/dt. \tag{1}$$

Using the normalization condition $p + \rho = 1$, its steady state solution can be obtained as follows

$$p = f/(f+w), \quad \rho = w/(f+w). \tag{2}$$

Let $U_{eff} = up + f\rho$, $W_{eff} = wp + b\rho$, then the mean velocity of cargo can be obtained as follows

$$\begin{aligned} V =&(U_{eff} - W_{eff})l_0 = [(u-w)p + (f-b)\rho]l_0 \\ =&(uf - wb)l_0/(f+w), \end{aligned} \tag{3}$$

where l_0 is the step size of cargo. The probabilities that cargo steps forward and backward are then

$$\begin{aligned} p_+ &= \frac{U_{eff}}{U_{eff} + W_{eff}} = \frac{f(u+w)}{f(u+w) + w(f+b)}, \\ p_- &= 1 - p_+ = \frac{w(f+b)}{f(u+w) + w(f+b)}. \end{aligned} \tag{4}$$

Finally, the external load F dependence of rate u, w, f, b can be given by the following Bell approximation [37–40],

$$\begin{aligned} u &= u_0 e^{-\epsilon_0 F l_0/k_B T}, \quad w = w_0 e^{(1-\epsilon_0)F l_0/k_B T}, \\ f &= f_0 e^{-\epsilon_1 F l_0/k_B T}, \quad b = b_0 e^{(1-\epsilon_1)F l_0/k_B T}. \end{aligned} \tag{5}$$

Where ϵ_0 and ϵ_1 are *load distribution factors* for the *plus-end* motor and *minus-end* motor, respectively. k_B is Boltzmann constant, and T is the absolute temperature. For more general study of the model given in Fig. 1(a), see [41]. In which both the expressions of mean velocity V and dispersion D are obtained.

B. Cargo Motion in one fixed optical trap

This special case is schematically depicted in Fig. 1(b). For convenience, the center of optical trap is assumed to be fixed at location 0. For this case, the potential of cargo depends on its location n. The potential difference between location n and location $n+1$ is $\Delta G_n = \kappa[(n+1)l_0]^2/2 - \kappa(nl_0)^2/2 = \kappa(n+1/2)l_0^2$. Similar as in [19], at location n, the forward and backward step rates u_n and w_n of cargo in *plus-state*, as well as the step rates f_n and b_n of cargo in *minus-state*, can be obtained as follows,

$$
\begin{aligned}
u_n &= ue^{-\epsilon_0 \Delta G_n/k_BT}, \quad w_n = we^{(1-\epsilon_0)\Delta G_{n-1}/k_BT}, \\
f_n &= fe^{-\epsilon_1 \Delta G_n/k_BT}, \quad b_n = be^{(1-\epsilon_1)\Delta G_{n-1}/k_BT}.
\end{aligned}
\tag{6}
$$

Where u, w, f, b are cargo step rates when there is no optical trap and any other external load, which satisfy $u \gg w, b \gg f$. For simplicity, this study assumes that ϵ_0, ϵ_1 are independent of cargo location n.

Let p_n, ρ_n be the probabilities of finding cargo in *plus-state* n^+ and *minus-state* n^-, respectively. One can easily show p_n, ρ_n are governed by the following equations

$$dp_n/dt = u_{n-1}p_{n-1} + f_{n-1}\rho_{n-1} - (u_n + w_n)p_n, \tag{7a}$$

$$d\rho_n/dt = w_{n+1}p_{n+1} + b_{n+1}\rho_{n+1} - (f_n + b_n)\rho_n. \tag{7b}$$

The steady state solution of Eqs. (7a, 7b) are as follows (for details see Sec. A of the supplemental materials [44])

$$p_n = \left[\prod_{k=0}^{n-1}\left(\frac{(f_k + b_k)u_k}{(u_{k+1} + w_{k+1})b_k}\right)\right] p_0, \quad \text{for } n \geq 1, \tag{8a}$$

$$p_n = \left[\prod_{k=n+1}^{0}\left(\frac{(u_k + w_k)b_{k-1}}{(f_{k-1} + b_{k-1})u_{k-1}}\right)\right] p_0, \quad \text{for } n \leq -1, \tag{8b}$$

$$\rho_n = \frac{u_n}{b_n}p_n = \frac{u_n}{b_n}\left[\prod_{k=0}^{n-1}\left(\frac{(f_k + b_k)u_k}{(u_{k+1} + w_{k+1})b_k}\right)\right] p_0, \tag{8c}$$

for $n \geq 1$,

$$\rho_n = \frac{u_n}{b_n}p_n = \frac{u_n}{b_n}\left[\prod_{k=n+1}^{0}\left(\frac{(u_k + w_k)b_{k-1}}{(f_{k-1} + b_{k-1})u_{k-1}}\right)\right] p_0, \tag{8d}$$

for $n \leq -1$,

$$\rho_0 = \frac{u_0}{b_0}p_0. \tag{8e}$$

Where p_0 can be obtained by the normalization condition $\sum_{n=-\infty}^{+\infty}(p_n + \rho_n) = 1$.

The probability of finding cargo in *plus-state* is $p = \sum_{n=-\infty}^{+\infty} p_n$, and the probability of finding cargo in *minus-state* is $\rho = \sum_{n=-\infty}^{+\infty} \rho_n$. The mean locations of cargo in *plus-state* and in *minus-state* are

$$\langle n^+\rangle = \sum_{n=-\infty}^{+\infty} np_n/p, \quad \langle n^-\rangle = \sum_{n=-\infty}^{+\infty} n\rho_n/\rho, \tag{9a}$$

respectively. The mean location of cargo is

$$\langle n\rangle = \sum_{n=-\infty}^{+\infty} n(p_n + \rho_n) = p\langle n^+\rangle + \rho\langle n^-\rangle. \tag{10}$$

Specially, for the *symmetric* cases $u = b, w = f$, i.e. the cargo is transported by two motors with the same step rates but different intrinsic directionality, one can verify that $\rho_n = p_{-n}$ and consequently $\rho = p, \langle n^- \rangle = -\langle n^+ \rangle, \langle n \rangle = 0$.

The external load dependence of rates u_n, w_n, f_n, b_n [see Eq. (6)] means that, for a cargo towed by two motors in one fixed optical trap there are two critical values of the cargo location n,

$$n_{c+} = \left\lceil \frac{k_B T}{\kappa l_0^2} \ln \frac{u}{w} + \frac{1}{2} - \epsilon_0 \right\rceil, \; n_{c-} = \left\lfloor \frac{k_B T}{\kappa l_0^2} \ln \frac{f}{b} + \frac{1}{2} - \epsilon_1 \right\rfloor, \tag{11}$$

where $\lceil x \rceil$ is the smallest integer number which is not less than x, $\lfloor x \rfloor$ is the biggest integer number which is not bigger than x. The step rates of *plus-end* motor satisfy $u_n > w_n$ for $n < n_{c+}$, and $u_n \le w_n$ for $n \ge n_{c+}$. Similarly, the step rates of *minus-end* motor satisfy $b_n > f_n$ for $n > n_{c-}$, and $b_n \le f_n$ for $n \le n_{c-}$. The intrinsic directionality of *plus-end* motor ($u \gg w$) implies $n_{c+} > 0$, and the intrinsic directionality of *minus-end* motor ($b \gg f$) implies $n_{c-} < 0$. Generally, the critical values n_{c+} and n_{c-} are different with the mean locations $\langle n^+ \rangle$ and $\langle n^- \rangle$.

In the following of this section, various mean first passage time (MFPT) problems about the cargo motion in fixed optical trap will be discussed.

1. *Mean first passage time to one of the plus-state*

Let t_n^l and τ_n^l be MFPTs of cargo from plus-state n^+ and minus-state n^- to plus-state l^+ respectively, then t_n^l and τ_n^l satisfy [42, 43]

$$w_n \tau_{n-1}^l - (u_n + w_n) t_n^l + u_n t_{n+1}^l = -1, \quad \text{for } n \neq l, \tag{12a}$$

$$b_n \tau_{n-1}^l - (f_n + b_n) \tau_n^l + f_n t_{n+1}^l = -1, \tag{12b}$$

with one boundary condition $t_l^l = 0$.

From Eq. (12a) one can easily get

$$\tau_{n-1}^l = \frac{u_n + w_n}{w_n} t_n^l - \frac{u_n}{w_n} t_{n+1}^l - \frac{1}{w_n}, \quad \text{for } n \neq l. \tag{13}$$

Substituting (13) into (12b), one obtains

$$\begin{aligned} & b_n \left[\frac{u_n + w_n}{w_n} t_n^l - \frac{u_n}{w_n} t_{n+1}^l - \frac{1}{w_n} \right] \\ & - (f_n + b_n) \left[\frac{u_{n+1} + w_{n+1}}{w_{n+1}} t_{n+1}^l - \frac{u_{n+1}}{w_{n+1}} t_{n+2}^l - \frac{1}{w_{n+1}} \right] \\ & + f_n t_{n+1}^l = -1, \end{aligned} \tag{14}$$

i.e.

$$B_n t_n^l - (B_n + F_n) t_{n+1}^l + F_n t_{n+2}^l = C_n, \tag{15}$$

where

$$\begin{aligned} B_n &= \frac{(u_n + w_n) b_n}{w_n}, \quad F_n = \frac{(f_n + b_n) u_{n+1}}{w_{n+1}}, \\ C_n &= \frac{b_n}{w_n} - \frac{f_n + b_n}{w_{n+1}} - 1. \end{aligned} \tag{16}$$

Note, Eqs. (14, 15) are established for $n \neq l-1, l$.

Meanwhile, from Eq. (12b) one can get

$$t_{n+1}^l = \frac{f_n + b_n}{f_n}\tau_n^l - \frac{b_n}{f_n}\tau_{n-1}^l - \frac{1}{f_n}, \tag{17}$$

and then by substituting Eq. (17) into Eq. (12a) one obtains

$$\begin{aligned} & w_n\tau_{n-1}^l - (u_n + w_n)\left[\frac{f_{n-1}+b_{n-1}}{f_{n-1}}\tau_{n-1}^l - \frac{b_{n-1}}{f_{n-1}}\tau_{n-2}^l - \frac{1}{f_{n-1}}\right] \\ & + u_n\left[\frac{f_n+b_n}{f_n}\tau_n^l - \frac{b_n}{f_n}\tau_{n-1}^l - \frac{1}{f_n}\right] = -1, \end{aligned} \tag{18}$$

i.e.

$$\hat{B}_n\tau_{n-2}^l - (\hat{B}_n + \hat{F}_n)\tau_{n-1}^l + \hat{F}_n\tau_n^l = \hat{C}_n, \tag{19}$$

where

$$\begin{aligned} \hat{B}_n &= \frac{(u_n + w_n)b_{n-1}}{f_{n-1}}, \quad \hat{F}_n = \frac{(f_n + b_n)u_n}{f_n}, \\ \hat{C}_n &= \frac{u_n}{f_n} - \frac{u_n + w_n}{f_{n-1}} - 1. \end{aligned} \tag{20}$$

Eqs. (18, 19) are established for $n \neq l$.

The procedure of getting MFPTs t_n^l, τ_n^l is as follows. **(1)** Getting t_n^l for $n \leq l-1$ by Eq. (15) and boundary condition $t_l^l = 0$ (see Sec. B of the supplemental materials [44]). **(2)** Getting τ_n^l for $n \leq l-2$ by Eq. (13). **(3)** Getting τ_{l-1}^l from the special case of Eq. (12b), i.e. $b_{l-1}\tau_{l-2}^l - (f_{l-1} + b_{l-1})\tau_{l-1}^l = -1$. **(4)** Getting τ_n^l for $n \geq l$ by Eq. (19) and boundary value τ_{l-1}^l obtained in **(3)** (see Sec. C of the supplemental materials [44]). **(5)** Getting t_n^l for $n \geq l+1$ by Eq. (17). This procedure can be summarized as follows

$$\begin{aligned} & \xrightarrow[t_l^l=0]{\text{Eq. (15)}} t_n^l(n \leq l-1) \xrightarrow{\text{Eq. (13)}} \tau_n^l(n \leq l-2) \\ & \xrightarrow[n=l-1]{\text{Eq. (12b)}} \tau_{l-1}^l \xrightarrow{\text{Eq. (19)}} \tau_n^l(n \geq l) \xrightarrow{\text{Eq. (17)}} t_n^l(n \geq l+1). \end{aligned} \tag{21}$$

2. Mean first passage time to one of the minus-state

Let $\bar{t}_n^l$ and $\bar{\tau}_n^l$ be the MFPTs of cargo from plus-state n^+ and minus-state n^- to minus-state l^-, respectively. Similar as the discussion in Sec. II B 1, the MFPTs $\bar{t}_n^l$ and $\bar{\tau}_n^l$ satisfy the following equations

$$w_n\bar{\tau}_{n-1}^l - (u_n + w_n)\bar{t}_n^l + u_n\bar{t}_{n+1}^l = -1, \tag{22a}$$

$$b_n\bar{\tau}_{n-1}^l - (f_n + b_n)\bar{\tau}_n^l + f_n\bar{t}_{n+1}^l = -1, \quad \text{for } n \neq l, \tag{22b}$$

with one boundary condition $\bar{\tau}_l^l = 0$. From Eq. (22a) one can easily get

$$\bar{\tau}_{n-1}^l = \frac{u_n + w_n}{w_n}\bar{t}_n^l - \frac{u_n}{w_n}\bar{t}_{n+1}^l - \frac{1}{w_n}. \tag{23}$$

Substituting (23) into (22b), one obtains

$$
\begin{aligned}
& b_n\left[\frac{u_n+w_n}{w_n}\bar{t}_n^l-\frac{u_n}{w_n}\bar{t}_{n+1}^l-\frac{1}{w_n}\right] \\
& -(f_n+b_n)\left[\frac{u_{n+1}+w_{n+1}}{w_{n+1}}\bar{t}_{n+1}^l-\frac{u_{n+1}}{w_{n+1}}\bar{t}_{n+2}^l-\frac{1}{w_{n+1}}\right] \\
& +f_n\bar{t}_{n+1}^l=-1,
\end{aligned}
\tag{24}
$$

i.e.

$$
B_n\bar{t}_n^l-(B_n+F_n)\bar{t}_{n+1}^l+F_n\bar{t}_{n+2}^l=C_n, \tag{25}
$$

with B_n, F_n, C_n given by Eq. (16). Note, Eqs. (24, 25) are established for $n \neq l$.

Meanwhile, from Eq. (22b) one can get

$$
\bar{t}_{n+1}^l=\frac{f_n+b_n}{f_n}\bar{\tau}_n^l-\frac{b_n}{f_n}\bar{\tau}_{n-1}^l-\frac{1}{f_n}, \quad \text{for } n\neq l, \tag{26}
$$

and then by substituting Eq. (26) into Eq. (22a) one obtains

$$
\begin{aligned}
& w_n\bar{\tau}_{n-1}^l-(u_n+w_n)\left[\frac{f_{n-1}+b_{n-1}}{f_{n-1}}\bar{\tau}_{n-1}^l-\frac{b_{n-1}}{f_{n-1}}\bar{\tau}_{n-2}^l-\frac{1}{f_{n-1}}\right] \\
& +u_n\left[\frac{f_n+b_n}{f_n}\bar{\tau}_n^l-\frac{b_n}{f_n}\bar{\tau}_{n-1}^l-\frac{1}{f_n}\right]=-1,
\end{aligned}
\tag{27}
$$

i.e.

$$
\hat{B}_n\bar{\tau}_{n-2}^l-(\hat{B}_n+\hat{F}_n)\bar{\tau}_{n-1}^l+\hat{F}_n\bar{\tau}_n^l=\hat{C}_n, \tag{28}
$$

with $\hat{B}_n, \hat{F}_n, \hat{C}_n$ given by Eq. (20). Eqs. (27, 28) are established for $n \neq l, l+1$.

The procedure of getting MFPTs $\bar{t}_n^l, \bar{\tau}_n^l$ is as follows. **(1)** Getting $\bar{\tau}_n^l$ for $n \geq l+1$ by Eq. (28) and boundary condition $\bar{\tau}_l^l=0$ (see Sec. D of the supplemental materials [44]). **(2)** Getting $\bar{t}_n^l$ for $n \geq l+2$ by Eq. (26). **(3)** Getting $\bar{t}_{l+1}^l$ from the special case of Eq. (22a), i.e. $-(u_{l+1}+w_{l+1})\bar{t}_{l+1}^l+u_{l+1}\bar{t}_{l+2}^l=-1$, **(4)** Getting $\bar{t}_n^l$ for $n \leq l$ by Eq. (25) with boundary value $\bar{t}_{l+1}$ obtained in **(3)** (see Sec. E of the supplemental materials [44]). **(5)** Getting $\bar{\tau}_n^l$ for $n \leq l-1$ by Eq. (23). This procedure can be summarized as follows

$$
\begin{aligned}
& \xrightarrow[\bar{\tau}_l^l=0]{\text{Eq. (28)}} \bar{\tau}_n^l(n\geq l+1) \xrightarrow{\text{Eq. (26)}} \bar{t}_n^l(n\geq l+2) \\
& \xrightarrow[n=l+1]{\text{Eq. (22a)}} \bar{t}_{l+1}^l \xrightarrow{\text{Eq. (25)}} \bar{t}_n^l(n\leq l) \xrightarrow{\text{Eq. (23)}} \bar{\tau}_n^l(n\leq l-1).
\end{aligned}
\tag{29}
$$

3. Mean first passage time to one given location

Let $\mathcal{T}_s^l$ be the MFPT of cargo from state s to location l (either *plus-state* l^+ or *minus-state* l^-), then one can easily show that

$$
\mathcal{T}_s^l=\begin{cases}
t_k^l, & \text{for } s=k^+ \ \text{ and } \ k<l, \\
\tau_k^l, & \text{for } s=k^- \ \text{ and } \ k<l, \\
\bar{t}_k^l, & \text{for } s=k^+ \ \text{ and } \ k>l, \\
\bar{\tau}_k^l, & \text{for } s=k^- \ \text{ and } \ k>l.
\end{cases}
\tag{30}
$$

It is to say that if $k < l$, a cargo located at k will first reach *plus-state* l^+ before reaching *minus-state* l^-. On the contrary, if $k > l$, it will first reach *minus-state* l^-. Finally, the mean oscillation period T of cargo in fixed optical trap can be approximated as follows

$$T \approx \tau_0^0 + \bar{t}_0^0, \tag{31}$$

see Sec. F of the supplemental materials for its expression [44].

III. RESULTS

For cargo motion under no external load, Monte Carlo simulations show that, if the cargo is transported by two *symmetric* motors, i.e., the *plus-end* motor and the *minus-end* motor have the same step rates, $u = b, w = f$, the cargo will oscillate [Fig. 2(a)]. While for the *asymmetric* cases, the cargo has non-zero mean velocity [see Fig. 2(b)]. On the other hand, if the cargo is put into one fixed optical trap, and transported by two *symmetric* motors, it will oscillate around the trap center with relatively high frequency [Fig. 2(c)]. Meanwhile, if the trapped cargo is transported by two *asymmetric* motors, it will also oscillate but its oscillation center may be different with the trap center [Fig. 2(d)]. Both Monte Carlo simulations and theoretical calculations show that, for a cargo transported by two *symmetric* motors and put in one optical trap, its oscillation period T decreases with trap stiffness κ, motor forward step rates $u = b$, and motor backward step rates $w = f$ [Fig. 3(a-c)]. Its oscillation amplitude increases with the motor forward step rates $u = b$, but decreases with both the motor backward step rates $u = b$ and the trap stiffness κ, since high backward step rates and high trap stiffness will prohibit the cargo from moving too far from the trap center [Fig. 3(d-f)].

Let

$$\begin{aligned} &p = \sum_{n=-\infty}^{\infty} p_n, \quad \rho = \sum_{n=-\infty}^{\infty} \rho_n, \\ &P_+ = \sum_{n>0} (p_n + \rho_n), \quad P_- = \sum_{n<0} (p_n + \rho_n). \end{aligned} \tag{32}$$

Then p is the probability of finding cargo in *plus-state*, P_+ is the probability that cargo location $n > 0$ (the center of optical trap is assumed to be at location 0). The meanings of ρ and P_- are similar. Both Monte Carlo simulations and theoretical calculations show that, for a cargo transported by two *symmetric* motors, the ratios p/ρ and P_+/P_- are always one, and they do not change with trap stiffness κ, forward step rates $u = b$, and backward step rates $w = f$ [Fig. S1].

Our results also show that, for cargo motion in optical trap by two *asymmetric* motors, its oscillation period T decreases with trap stiffness κ and forward step rate u, but may not change monotonically with backward step rate w [Figs. S2(a), S3(a), S4(a)]. But similar as the *symmetric* cases, cargo oscillation amplitude of the *asymmetric* cases decreases with trap stiffness κ and backward step rate w, and increases with the forward step rate u [Figs. S2(d), S3(d), S4(d)]. The results in Figs. S3(d), and S4(d) imply that, the maximal location $n_{\max}$ that cargo might reach toward the *plus-end* of microtubule depends only on the step rates u, w of the *plus-end* motor, and similarly the minimal location $n_{\min}$ that cargo might reach towards the *minus-end* of the microtubule depends only on the step rates b, f of the *minus-end* motor. From the results given in Figs. S2(b,c), S3(b,c), and S4(b,c) one can also see that, different from the *symmetric* cases given in Fig. S1, both the ratio p/ρ and ratio P_+/P_- depend on trap stiffness κ, forward step rate u, and backward step rate w.

To show more details about the dependence of cargo oscillation on trap stiffness κ and motor step rates, examples of probabilities p_n, ρ, and their summation $p_n + \rho_n$ are plotted in Fig. 4 and Fig. S5. For either *symmetric* cases or *asymmetric* cases, the probability profiles are flat for low trap stiffness κ, indicating that the cargo can reach a farther location from the oscillation center (i.e., with large oscillation amplitude)[Fig. S5]. Similar changes can also be found with the increase of motor forward step rates u or f [Fig. 4(a, b, d)]. Meanwhile, with the increase of motor backward step rates w or f, the probability profile will become more sharp [Fig. 4(c)]. For the *asymmetric* cases, the most likely location of cargo may be different from the trap center [Fig. S5(c)]. One interesting phenomenon displayed in Fig. 4(b, d) is that, for either the *symmetric* cases or the *asymmetric* cases, when motor forward step rates u, b are high, the summation of probability $p_n + \rho_n$ may has two local maxima, indicating that cargo motion in the positive location ($n > 0$) is mainly dominated by the plus motor, while its motion in the negative location ($n < 0$) is mainly dominated by the minus motor.

Let $N_{\max p_n}, N_{\max \rho_n}, N_{(p_n+\rho_n)_{\max}}$ be the locations at which probabilities p_n, ρ_n and their summation $p_n + \rho_n$ reach their maxima, respectively. The results plotted in Fig. 5(a) show that, for *symmetric* motion, $N_{\max \rho_n} = -N_{\max p_n}$ and their absolute values increase with the forward to backward step rate ratio $u/w = b/f$. The results in Fig. 5(d) show that, for low step rate ratio $u/w = b/f$, the total probability $p_n + \rho_n$ has only one maximum which lies at the trap center. However, with increase of these ratios, $N_{(p_n+\rho_n)_{\max}}$ has one *symmetric* bifurcation, and its absolute value (see Fig. 4) increases with these step ratios. For *asymmetric* case [see Fig. 5(b)], $N_{\max p_n}$ increases with step rate ratio u/w, but $N_{\max \rho_n}$ is independent of it. Which means that, similar as the properties of $n_{\max}$ and $n_{\min}$ displayed in Figs. S3 and S4, $N_{\max p_n}$ depends only on step rates of the *plus-end* motor, and $N_{\max \rho_n}$ depends only on step rates of the *minus-end* motor. For *asymmetric* cases, with the increase of rate ratio u/w, $N_{(p_n+\rho_n)_{\max}}$ has also one bifurcation, see Fig. 5(e). But one of the two values (the negative one) does not change with u/w. Which means that, the negative one of $N_{(p_n+\rho_n)_{\max}}$ depends only on properties of the *minus-end* motor. Similarly, the positive one of $N_{(p_n+\rho_n)_{\max}}$ depends only on properties of the *plus-end* motor. So both the properties of amplitude $n_{\max}, n_{\min}$ and the most likely locations $N_{\max p_n}, N_{\max \rho_n}, N_{(p_n+\rho_n)_{\max}}$ indicate that, the *plus-end* directed motion of cargo is mainly determined by the *plus-end* motor, and the *minus-end* directed motion is mainly determined by the *minus-end* motor, which is one of the main differences with other tug-of-war models [14, 18, 19, 21], and this result is consistent with the experimental phenomena [15, 16, 36]. Finally, the results in Fig. 5(c) show that, the absolute values of $N_{\max p_n}, N_{\max \rho_n}$ decrease with trap stiffness κ, and Fig. 5(f) shows $N_{(p_n+\rho_n)_{\max}}$ does not change with stiffness κ. So trap stiffness can change the oscillation amplitude and the oscillation period (see Figs. 3, S2, and S5), but will not change the most likely location $N_{(p_n+\rho_n)_{\max}}$ of the cargo. Further calculations of probabilities p, ρ show that, for the *symmetric* cases both $p_{\max} = \rho_{\min}$ and $(p + \rho)_{\min}$ decrease with step rate ratio $u/w = b/f$, and increase with trap stiffness κ [see Figs. S6(a,d)]. Since with large rate ratio $u/w = b/f$ and small stiffness κ, the cargo will oscillate with large amplitude. For the *asymmetric* cases, $p_{\max} \neq \rho_{\min}$, $p_{\max}$ decreases but $\rho_{\min}$ increases with the step rate ratio u/w (i.e. with the increase of the directionality of the *plus-end* motor). Since with large rate ratio u/w, the *plus-end* motor has high directionality, and so the cargo moves fast in the *plus-state*, which means that the probability p_n will be flat with large u/w. The plots in Fig. S6(c) show that, although the total probability $p_n + \rho_n$ has two maxima, with the change of rate ratio u/w, the most likely location of cargo may change from one side of the trap center to another side.

Finally, several examples of MFPTs $t_n^l, \tau_n^l, \bar{t}_n^l, \bar{\tau}_n^l$ are plotted in Fig. 6(a,b) and Figs. S7, S8(a,b), S9-S12, and examples of MFPTs $\mathcal{T}_{n\pm}^l$ are plotted in Fig. 6(c,d) and Fig. S8(c,d). If $m < n < l$, then $t_n^l \le t_m^l, \tau_m^l \le \tau_n^l$, $\bar{t}_n^l \le \bar{t}_m^l, \bar{\tau}_m^l \le \bar{\tau}_n^l$, and $\mathcal{T}_{n+}^l \le \mathcal{T}_{m+}^l, \mathcal{T}_{m-}^l \le \mathcal{T}_{n-}^l$. If $l < n < m$, then $t_n^l \ge t_m^l, \tau_m^l \ge \tau_n^l$, $\bar{t}_n^l \ge \bar{t}_m^l, \bar{\tau}_m^l \ge \bar{\tau}_n^l$, and $\mathcal{T}_{n+}^l \ge \mathcal{T}_{m+}^l, \mathcal{T}_{m-}^l \ge \mathcal{T}_{n-}^l$. Moreover, if the trap stiffness κ is high and the motor step rate ratios u/w and b/f are large, then $t_m^l \le \tau_m^l, \bar{t}_m^l \le \bar{\tau}_m^l$, $\mathcal{T}_{m+}^l \le \mathcal{T}_{m-}^l$ for $m < n < l$, and $t_m^l \ge \tau_m^l, \bar{t}_m^l \ge \bar{\tau}_m^l$, $\mathcal{T}_{m+}^l \ge \mathcal{T}_{m-}^l$ for $l < n < m$, see Fig. 6(a,c,d) and Figs. S7(a,b), S8(c,d),S9, S10(a), S11(b,c,d), S12(a).

IV. DISCUSSION

Recent experimental observations by Leidel *et al.* [36] show that, in living cells cargo moves along microtubule with memory, i.e., its motion direction depends on its previous motion trajectory. In this study, such cargo transportation is theoretically studied by assuming that the cargo has the least memory, i.e. its motion direction depends only on its behavior in its last step. The cargo will be more likely to step forward/backward if it came to its present location by one forward/backward step. Two cases are mainly discussed: **(I)** cargo moves under constant load, and **(II)** cargo moves in one fixed optical trap. For each cases, two kinds of motion are addressed: **(i)** *symmetric* motion, in which cargo is transported by two types of motor protein which have the same forward/backward step rates but with different intrinsic directionality, **(ii)** *asymmetric* motion, in which cargo is transported by two types of motor protein with different forward/backward step rates. For the *symmetric* motion **(i)** of case **(I)**, the mean velocity of cargo is zero. But, due to the existence of memory, cargo can move unidirectionally for a large distance before switching its direction. One can easily understand that, for the *asymmetric* motion **(ii)** of **(I)**, the directionality of cargo with memory is better than that in the usual tug-of-war model by two different motor types [14, 19, 21]. For the motion in one fixed optical trap, i.e. case **(II)**, cargo will oscillate. For the *symmetric* motion **(i)**, the oscillation center is the same as the trap center, but for the *asymmetric* motion **(ii)** , this oscillation center is generally different from the trap center. Usually the oscillation period decreases with the trap stiffness κ and motor step rates. Meanwhile, the oscillation amplitude decreases with trap stiffness κ and motor backward step rates w, f, but increases with motor forward step rates u, b. The probability $p_n + \rho_n$ of finding cargo at location n may have only one maximum, which is the same as the trap center for *symmetric* motion **(i)** but different with the trap center for *asymmetric* motion **(ii)**. Meanwhile, the probability $p_n + \rho_n$ may also have two maxima. For *symmetric* motion **(i)**, these two maxima are located symmetrically on the two side of the trap center, and their corresponding values of probability $p_n + \rho_n$ are the same. However, for the *asymmetric* motion **(ii)**, these two maxima are generally not symmetrically located around the trap center, and their corresponding probabilities may be greatly different. With the change of ratio of motor forward to backward step rates, the maximum with the larger value of probability $p_n + \rho_n$ may transfer from one side of the trap center to another side. Mathematically, the model used in this study is similar as the one used in [40] to describe the dynamic properties of microtubule (see Fig. S13 in the supplementary Materials [44]). This study will be helpful to understand the high directionality of cargo motion in living cells by cooperation of two types of motor protein. Meanwhile, more generalized model can also be employed to discuss this cargo transportation process, in which the cargo is assumed to have long memory, its forward and backward step rates depend on how long it has kept moving in its present direction.

Acknowledgments

This study was supported by the Natural Science Foundation of China (Grant No. 11271083), Natural Science Foundation of Shanghai (Grant No. 11ZR1403700), and the National Basic Research Program of China (National "973" program, project No. 2011CBA00804).

[1] D. Bray. *Cell movements: from molecules to motility, 2nd Edn.* Garland, New York, 2001.

[2] J. Howard. *Mechanics of Motor Proteins and the Cytoskeleton.* Sinauer Associates and Sunderland, MA, 2001.

[3] S. M. Block, L. S. B. Goldstein, and B. J. Schnapp. Bead movement by single kinesin molecules studied with optical tweezers. *Nature*, 348:348–352, 1990.

[4] R. D. Vale. The molecular motor toolbox for intracellular transport. *Cell*, 112:467–480, 2003.

[5] R. Mallik, B. C. Carter, S. A. Lex, S. J. King, and S. P. Gross. Cytoplasmic dynein functions as a gear in response to load. *Nature*, 427:649–652, 2004.

[6] W. Hua, Edgar C. Young, Margaret L. Fleming, and Jeff Gelles. Coupling of kinesin steps to ATP hydrolysis. *Nature*, 388:390–393, 1997.

[7] Mark J. Schnitzer and Steven M. Block. Kinesin hydrolyses one ATP per 8-nm step. *Nature*, 388:386–390, 1997.

[8] D. L. Coy, M. Wagenbach, and J. Howard. Kinesin takes one 8-nm step for each ATP that it hydrolyzes. *J. Biol. Chem.*, 274:3667–3671, 1999.

[9] Arne Gennerich, Andrew P. Carter, Samara L. Reck-Peterson, and Ronald D. Vale. Force-induced bidirectional stepping of cytoplasmic dynein. *Cell*, 131:952–965, 2007.

[10] Charles L. Asbury, Adrian N. Fehr, and Steven M. Block. Kinesin moves by an asymmetric hand-over-hand mechanism. *Science*, 302:2130–2134, 2003.

[11] S. Toba, T. M. Watanabe, L. Yamaguchi-Okimoto, Y. Y. Toyoshima, and H. Higuchi. Overlapping hand-over-hand mechanism of single molecular motility of cytoplasmic dynein. *Proc. Natl. Acad. Sci. USA*, 103:5741–5745, 2006.

[12] N. R. Guydosh and S. M. Block. Direct observation of the binding state of the kinesin head to the microtubule. *Nature*, 461:125–128, 2009.

[13] Stefan Klumpp and Reinhard Lipowsky. Cooperative cargo transport by several molecular motors. *Proc. Natl. Acad. Sci. USA*, 102:17284–17289, 2005.

[14] M. J. I. Müller, S. Klumpp, and R. Lipowsky. Tug-of-war as a cooperative mechanism for bidirectional cargo transport by molecular motors. *Proc. Natl. Acad. Sci. USA*, 105:4609–4614, 2008.

[15] A. Gennerich and D. Schild. Finite-particle tracking reveals sub-microscopic size changes of mitochondria during transport in mitral cell dendrites. *Phys. Biol. 3:45-53*, 3:45–53, 2006.

[16] V. Soppina, A. K. Rai, A. J. Ramaiya, P. Barak, and R. Mallik. Tug-of-war between dissimilar teams of microtubule motors regulates transport and fission of endosomes. *Proc. Natl. Acad. Sci. USA*, 106:19381–19386, 2009.

[17] A. Kunwar, M. Vershinin, J. Xu, and S. P. Gross. Stepping, strain gating, and an unexpected force-velocity curve for multiple-motor-based transport. *Curr. Biol.*, 18:1173–1183, 2008.

[18] A. Kunwar and A. Mogilner. Robust transport by multiple motors with nonlinear force-velocity relations and stochastic load sharing. *Phys. Biol.*, 7:016012, 2010.

[19] Yunxin Zhang. Cargo transport by several motors. *Phys. Rev. E*, 83:011909, 2011.

[20] A. R. Rogers, J. W. Driver, P. E. Constantinou, D. K. Jamison, and M. R. Diehl. Negative interference dominates collective

transport of kinesin motors in the absence of load. *Phys. Chem. Chem. Phys.*, 11:4882, 2009.

[21] J.W. Driver, A.R. Rogers, D.K. Jamison, R.K. Das, A.B. Kolomeisky, and M.R. Diehl. Coupling between motor proteins determines dynamic behaviors of motor protein assemblies. *Phys. Chem. Chem. Phys.*, 12:10398–10405, 2010.

[22] J. W. Driver, D. K. Jamison, K. Uppulury, A. R. Rogers, A. Kolomeisky, and M. R. Diehl. Productive cooperation among processive motors depends inversely on their mechanochemical efficiency. *Biophys. J.*, 101:386–395, 2011.

[23] D. K. Jamison, J. W. Driver, and M. R. Diehl. Cooperative responses of multiple kinesins to variable and constant loads. *J. Biol. Chem.*, 287:3357–3365, 2011.

[24] K. Uppulury, A. K. Efremov, J. W. Driver, D. K. Jamison, M. R. Diehl, and A. Kolomeisky. How the interplay between mechanical and non-mechanical interactions affect multiple kinesin dynamics. *J. Phys. Chem. B*, 116:8846–8855, 2012.

[25] A. Kunwar, S. K. Tripathy, J. Xu, M. Mattson, R. Sigua, R. McKinney, C. Yu, A. Mogilner, and S. P. Gross. Mechanical stochastic tug-of-war models cannot explain bidirectional lipid-droplet transport. *Proc. Natl. Acad. Sci. USA*, 108:18960–18965, 2011.

[26] S. Bouzat, V. Levi, and L. Bruno. Transport properties of melanosomes along microtubules interpreted by a tug-of-war model with loose mechanical coupling. *PLoS ONE*, 7:e43599, 2012.

[27] F. Jülicher and J. Prost. Cooperative molecular motors. *Phys. Rev. Lett.*, 75:2618–2621, 1995.

[28] M. Badoual, F. Jülicher, and J. Prost. Bidirectional cooperative motion of molecular motors. *Proc. Natl. Acad. Sci. USA*, 99:6696–6701, 2002.

[29] K. Adachi, K. Oiwa, T. Nishizaka, S. Furuike, H. Noji, H. Itoh, M. Yoshida, and Jr. K. Kinosita. Coupling of rotation and catalysis in F_1-ATPase revealed by single-molecule imaging and manipulation. *Cell*, 130:309–321, 2007.

[30] Peter Bieling, Ivo A. Telley, Jacob Piehler, and Thomas Surrey. Processive kinesins require loose mechanical coupling for efficient collective motility. *EMBO Reports*, 19:1121–1127, 2008.

[31] R. Mallik and S. P. Gross. Intracellular transport: How do motors work together? *Curr. Biol.*, 19:R416–R418, 2009.

[32] G. J. Brouhard. Motor proteins: Kinesins influence each other through load. *Curr. Biol.*, 20:R448–R450, 2010.

[33] M. A. Welte. Bidirectional transport: Matchmaking for motors. *Curr. Biol.*, 20:R410–R413, 2010.

[34] Adam G. Hendricks, Eran Perlson, Jennifer L. Ross, Harry W. Schroeder, Mariko Tokito, and Erika L.F. Holzbaur. Motor coordination via a tug-of-war mechanism drives bidirectional vesicle transport. *Current Biology*, 20:697–702, 2010.

[35] H. W. Schroeder, C. Mitchell, H. Shuman, E. L. F. Holzbaur, and Y. E. Goldman. Motor number controls cargo switching at actin-microtubule intersections in vitro. *Curr. Biol.*, 20:687–696, 2010.

[36] C. Leidel, R. A. Longoria, F. M. Gutierrez, and G. T. Shubeita. Measuring molecular motor forces in vivo: Implications for tug-of-war models of bidirectional transport. *Biophys. J.*, 103:492–500, 2012.

[37] George I. Bell. Models for the specific adhesion of cells to cells. *Science*, 200:618–627, 1978.

[38] M. E. Fisher and A. B. Kolomeisky. Simple mechanochemistry describes the dynamics of kinesin molecules. *Proc. Natl. Acad. Sci. USA*, 98:7748–7753, 2001.

[39] Y. Zhang. A general two-cycle network model of molecular motors. *Physica A*, 383:3465–3474, 2009.

[40] Y. Zhang. Growth and shortening of microtubules: A two-state model approach. *J. Biol. Chem.*, 286:39439–39449, 2011.

[41] Evgeny B. Stukalin and Anatoly B. Kolomeisky. Transport of single molecules along the periodic parallel lattices with coupling. *J. Chem. Phys.*, 124:204901, 2006.

[42] S. Redner. *A Guide to First-Passage Processes*. Cambridge University Press, 2001.

[43] Yunxin Zhang. Periodic one-dimensional hopping model with transitions between nonadjacent states. *Phys. Rev. E*, 84:031104, 2011.

[44] See Supplementary Material Document No.__ for more figures and calculations of various mean first passages.

TABLE I: The values of rates u, w, f, b (in unit s^{-1}) and optical trap stiffness κ (pN/nm) used in the plots of Figs. 2-6. The symbol $*$ means that the corresponding parameter is not used in the plot, and symbol $\surd$ means this parameter is one variable in the corresponding plot. Other parameters used in the plots are $\epsilon_0 = \epsilon_1 = 0.5$, $l_0 = 8$ nm, and $k_B T = 4.12$ pN·nm. The stiffness κ of the trap used in recent experiment of Leidel *el al.* is around $0.02 - 0.09$ pN/nm [36].

	u	w	f	b	κ
Fig. 2(a)	5	2	2	5	$*$
Fig. 2(b)	5	2	1	2	$*$
Fig. 2(c)	20	1	1	20	0.004
Fig. 2(d)	20	1	1	5	0.001
Fig. 3(a,d)	10	1	1	10	$\surd$
Fig. 3(b,e)	$\surd$	1	1	$\surd$	0.05
Fig. 4(c,f)	100	$\surd$	$\surd$	100	0.05
Fig. 4(a)	10	1	1	10	0.05
Fig. 4(b)	50	1	1	50	0.05
Fig. 4(c)	20	15	15	20	0.05
Fig. 4(d)	50	1	1	30	0.05
Fig. 5(a,d)	$\surd$	1	1	$\surd$	0.05
Fig. 5(b,e)	$\surd$	1	1	50	0.05
Fig. 5(c,f)	10	1	1	10	$\surd$
Fig. 6(a)	5	1	1	5	0.05
Fig. 6(b)	5	1	1	5	0.01
Fig. 6(c)	30	1	1	10	0.05
Fig. 6(d)	10	1	1	10	0.05

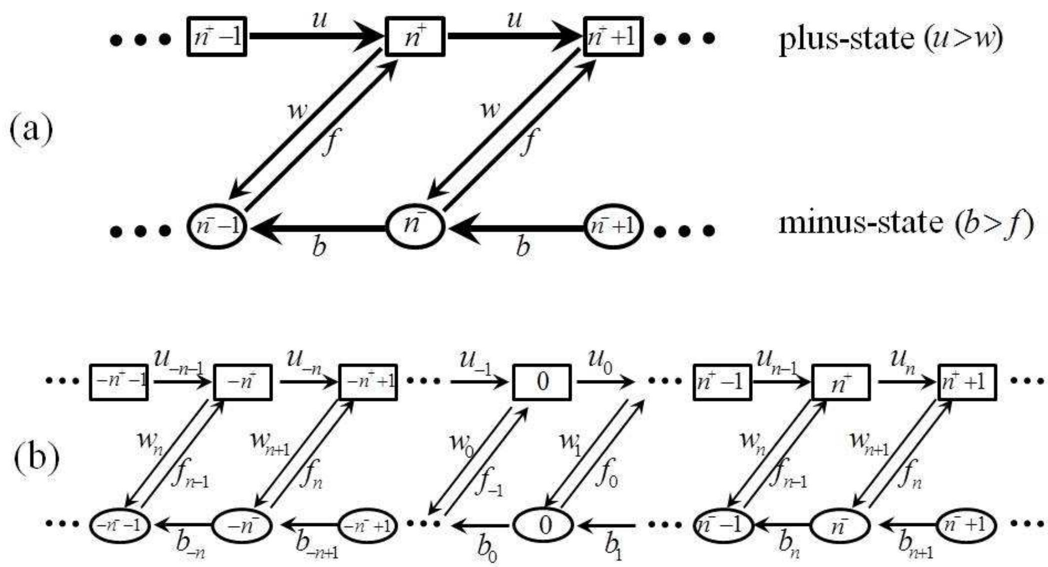

FIG. 1: Schematic depiction of the model discussed in this study to explain the cargo motion with memory. (a) is for cargo motion under constant load, and (b) is for cargo motion in one fixed optical trap. At any location n, the cargo may be in two different states, *plus-state* n^+ and *minus-state* n^-. Cargo in *plus-state* n^+ means it reaches location n from location $n-1$, while cargo in *minus-state* means it is from location $n+1$. For a cargo in *plus-state* n^+, its forward and backward step rates are u and w respectively. But for a cargo in *minus-state* n^-, it has different step rates f and b. For the constant load cases (a), $u > w$ and $b > f$ mean that, if the cargo is in *plus-state* n^+ it will be more likely to move forward to location $n+1$. Otherwise, it will be more likely to move backward to location $n-1$.

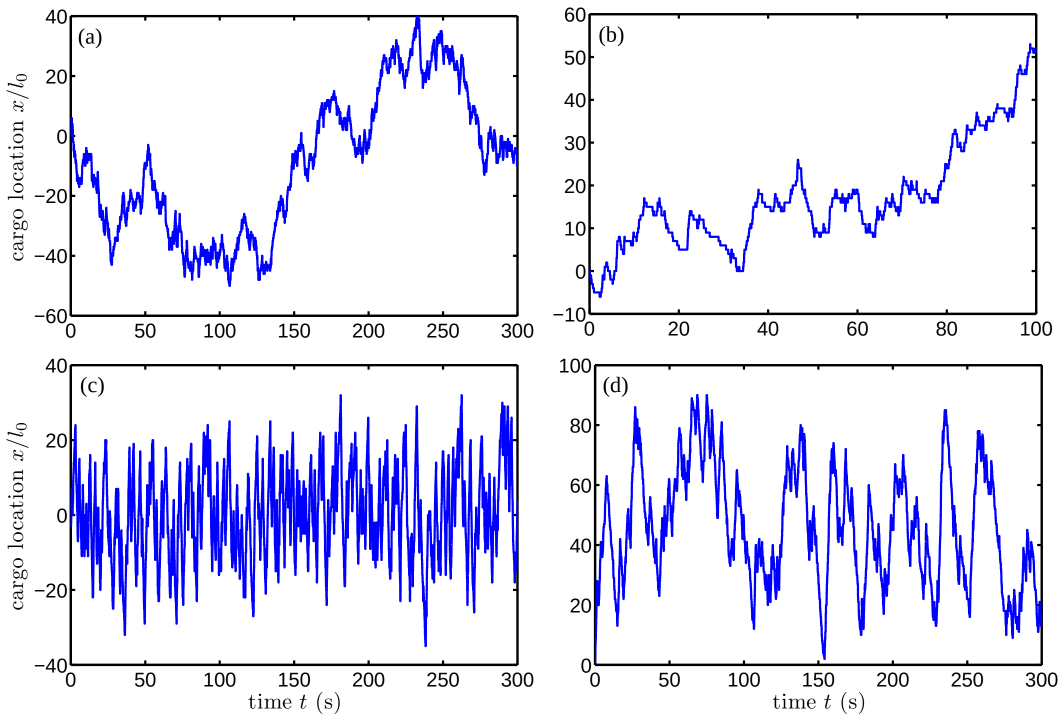

FIG. 2: Trajectory samples of cargo motion by two motors under constant load (a, b), and in one fixed optical trap (c, d). For the symmetric cases (where the step rates of the plus motor are the same as the ones of the minus motor, i.e. $u = b$, $w = f$), the cargo will oscillate around its initial location (a). While for the asymmetric cases, the cargo will have nonzero mean velocity (b). If the cargo is put in one fixed optical trap and transported by two *symmetric* motors, it will oscillate around the trap center (c). But for the asymmetric cases, the oscillation center may be different from the trap center. For parameter values used in the simulations see Tab. I.

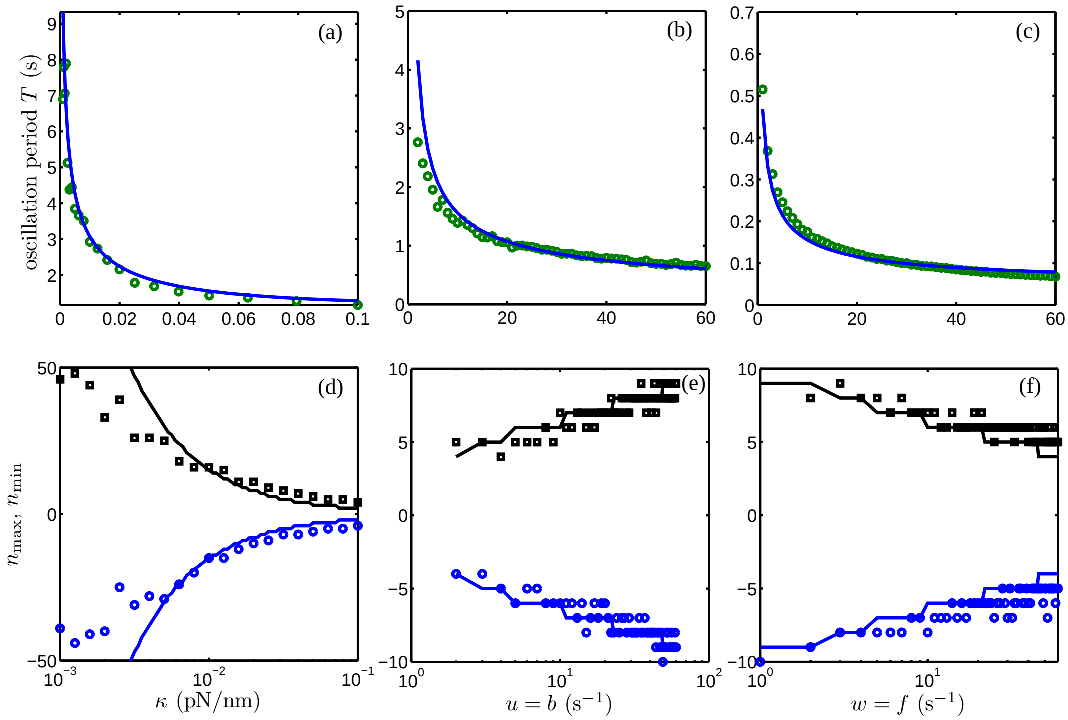

FIG. 3: In fixed optical trap, the mean oscillation period T of cargo decreases with trap stiffness κ, forward rates $u = b$, and backward rates $w = f$ (in fact, $\log T$ decreases almost linearly with $\log \kappa$, $\log u = \log b$, and $\log w = \log f$). The oscillation amplitude $n_{\max} - n_{\min}$ decreases with stiffness κ and backward rates $w = f$, but increases with forward rates $u = b$. Here $n_{\max}$ and $n_{\min}$ are the max and min locations that cargo can reaches. The circles and squares are obtained by Monte Carlo simulations. In (a, b, c), the solid curves are obtained by formulation (31). The solid lines in (d) are obtained by n_{c+}, n_{c-} given in Eq. (11), and the solid lines in (e, f) are obtained by $n_{c+} + 3, n_{c-} - 3$, respectively. For parameter values see Tab. I.

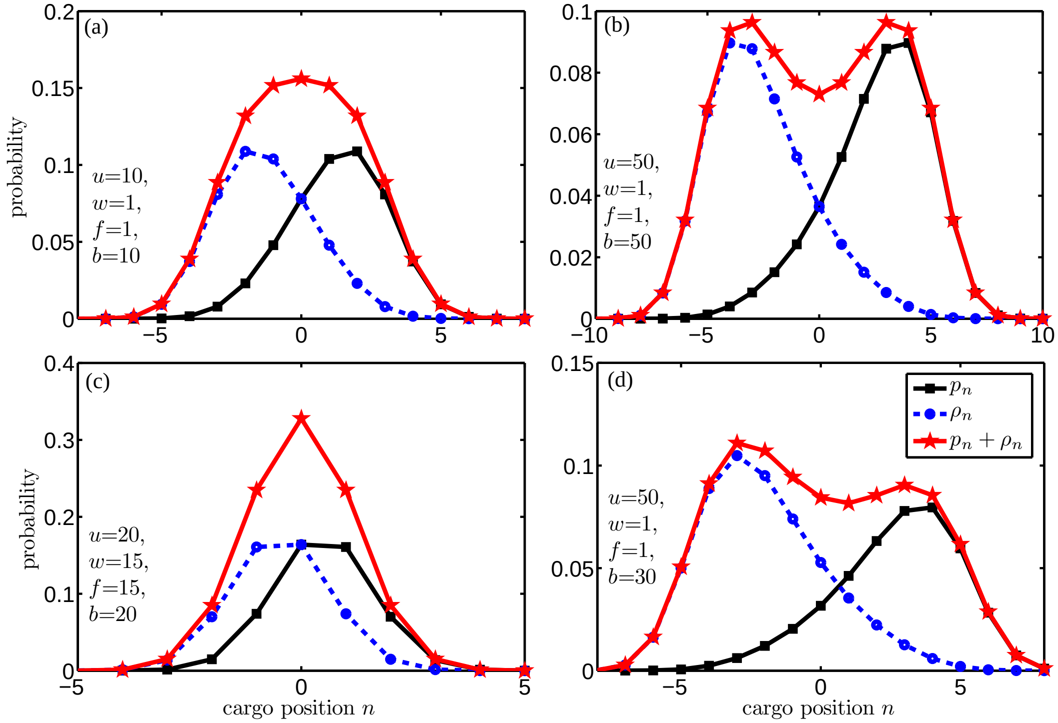

FIG. 4: Samples of probability p_n and ρ_n for finding cargo in *plus-state* and *minus-state*. For the symmetric cases probabilities p_n and ρ_n are mirror symmetry to each other (a, b, c). Their sum $p_n + \rho_n$, the probability of finding cargo at location n, might has one maximum [at the center of optical trap, see (a, c)] or two symmetric maximum [see (b)]. (d) is one sample for the asymmetric cases. For parameter values see Tab. I.

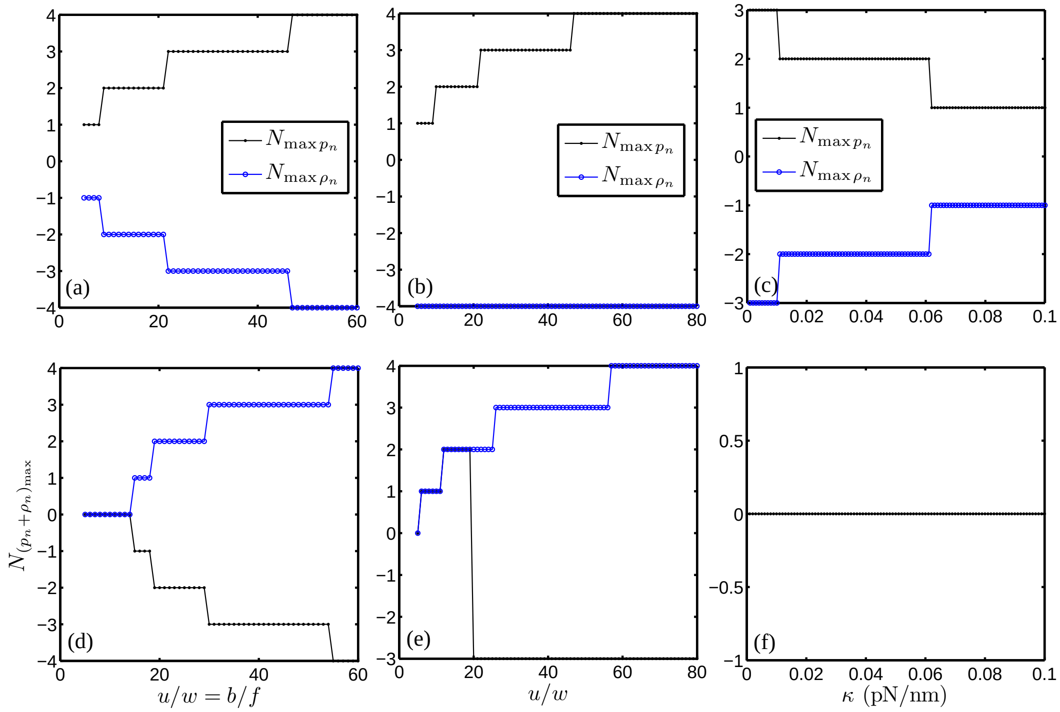

FIG. 5: The location $N_{\max p_n}, N_{\max \rho_n}, N_{(p_n+\rho_n)_{\max}}$ that probabilities p_n, ρ_n and their summation $p_n+\rho_n$ reach their maximum. With the increase of rate ratio $u/w = b/f$ both $N_{\max p_n}$ and $N_{\max \rho_n}$ leave far away from the trap center (a). (b) implies that $N_{\max p_n}$ increases with ratio u/w, but $N_{\max \rho_n}$ is independent of it. With the increase of trap stiffness κ, both $N_{\max p_n}$ and $N_{\max \rho_n}$ come close the the trap center (c). (d, e) show that, with the increase of rate ratio $u/w = b/f$ or rate ratio u/w only, the number of maximum of probability $p_n + \rho_n$ of finding cargo at location n may change. But (f) implies that $N_{(p_n+\rho_n)_{\max}}$ is independent of trap stiffness κ. For parameter values see Tab. I.

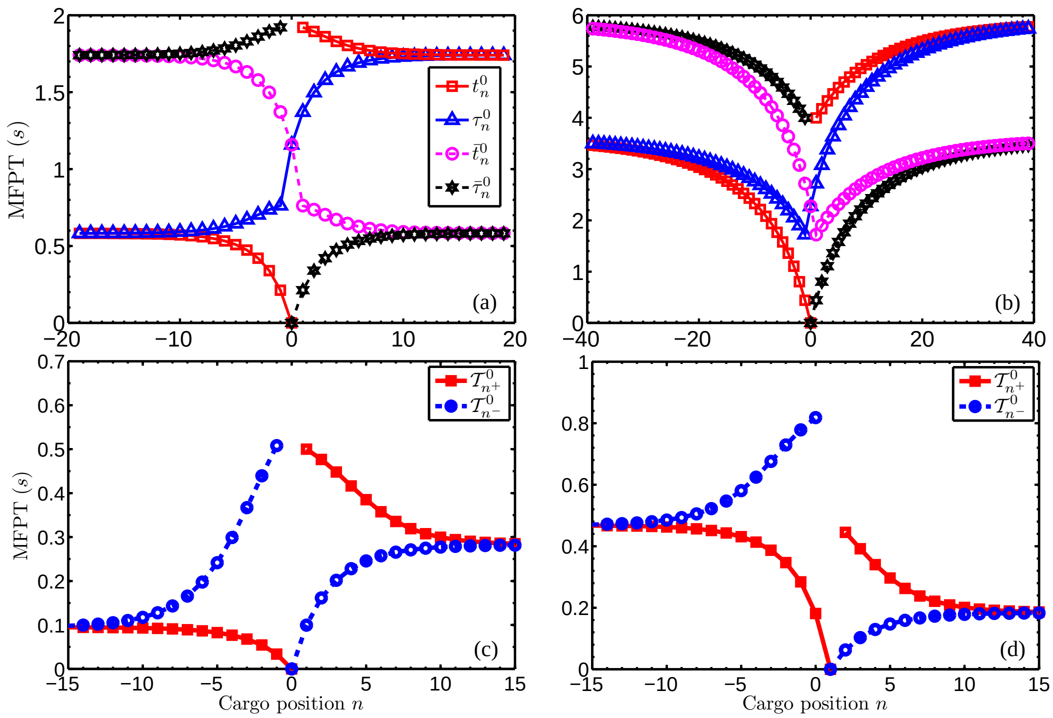

FIG. 6: Samples of MFPTs t_n^0, τ_n^0 to *plus-state* 0^+, MFPTs $\bar{t}_n^0, \bar{\tau}_n^0$ to *minus-state* 0^- (a, b), and MFPT $\mathcal{T}_l^0$ from state l to location 0 (c, d). For high trap stiffness κ, $t_{n<0}^0 < \tau_{m<0}^0 < \tau_{l\geq 0}^0 < t_{k>0}^0$ for MPFTs to *plus-state* 0^+, and symmetric relations hold for MFPTs to *minus-state* 0^-, see (a). But for low trap stiffness, all MFPTs $t_n^0, \tau_n^0, \bar{t}_n^0, \bar{\tau}_n^0$ increases with the distance between n and trap center 0, see (b). Which means that, for different trap stiffness κ, the trajectories of cargo from state n^+ or n^- to state 0^+ or 0^- are different. (c, d) are MFPTs for one cargo (transported by two *asymmetric* motors) from state n^+ or n^- to location 0 (*plus-state* 0^+ or 0^-) and location 1 (*plus-state* 1^+ or 1^-). The MFPT $\mathcal{T}_n^0$ is obtained by formulation (30). For parameter values see Tab. I.